atmosphere

MDPI

Article

Spatio-Temporal Variability in North Atlantic Oscillation Monthly Rainfall Signatures in Great Britain

Harry West *, Nevil Quinn and Michael Horswell

Centre for Water, Communities and Resilience, Department of Geography and Environmental Management, University of the West of England, Bristol BS16 1QY, UK; Nevil.Quinn@uwe.ac.uk (N.Q.); michael.horswell@uwe.ac.uk (M.H.)

* Correspondence: harry.west@uwe.ac.uk

Abstract: The North Atlantic Oscillation (NAO) is the primary atmospheric-oceanic circulation/teleconnection influencing regional climate in Great Britain. As our ability to predict the NAO several months in advance increases, it is important that we improve our spatio-temporal understanding of the rainfall signatures that the circulation produces. We undertake a high resolution spatio-temporal analysis quantifying variability in rainfall response to the NAO across Great Britain. We analyse and map monthly NAO-rainfall response variability, revealing the spatial influence of the NAO on rainfall distributions, and particularly the probability of wet and dry conditions/extremes. During the winter months, we identify spatial differences in the rainfall response to the NAO between the NW and SE areas of Britain. The NW area shows a strong and more consistent NAO-rainfall response, with greater probability of more extreme wet/dry conditions. However, greater NAO-rainfall variability during winter was found in the SE. The summer months are marked by a more spatially consistent rainfall response; however, we find that there is variability in both wet/dry magnitude and directionality. We note the implications of these spatially and temporally variable NAO-rainfall responses for regional hydrometeorological predictions and highlight the potential explanatory role of other atmospheric-oceanic circulations.

Keywords: North Atlantic Oscillation; NAO; rainfall signatures; spatio-temporal analysis

Citation: West, H.; Quinn, N.; Horswell, M. Spatio-Temporal Variability in North Atlantic Oscillation Monthly Rainfall Signatures in Great Britain. *Atmosphere* **2021**, *12*, 763. https://doi.org/10.3390/atmos12060763

Academic Editors: Ankit Agarwal, Naiming Yuan, Kevin K. W. Cheung and Roopam Shukla

Received: 15 May 2021
Accepted: 11 June 2021
Published: 13 June 2021

1. Introduction

Weather in Great Britain can be highly variable, fluctuating between wet and dry extremes. The North Atlantic Oscillation (NAO) atmospheric-oceanic circulation has long been cited as the leading mode of climate variability in the North Atlantic region [1–3] due to its influence on the location and amplitude of the North Atlantic Jet Stream [4]. The NAO teleconnection is commonly defined by the sea level pressure (SLP) variation between two meridional dipoles: the Icelandic low-pressure action point and the Azores anticyclone. Fluctuations in the difference in SLP between Iceland and the Azores leads to the occurrence of NAO positive (NAO+) phases, representing a greater than normal difference in SLP between the two dipoles, or NAO negative (NAO−) phases representing a weaker than normal difference in SLP. The strength and phase of the NAO can be quantified by the North Atlantic Oscillation Index (NAOI) [3].

Previous work has explored the influence of sub-annual variability and phase of the NAO on weather and climate in Great Britain. Strong positive correlations are often reported between the NAOI and winter rainfall in the north-western areas of the country [5–7], whilst weaker negative winter correlations have been found in the south-east and central areas [8,9]. Previous work has quantified these opposing regional rainfall responses to NAO+ and NAO− phases relative to when the NAO is in a weak neutral state, finding that in winter, average monthly rainfall increases under NAO+ and decreases under NAO− conditions can be as much as 200–300 mm in the north-west [10]. Negative correlations between the winter NAOI and modelled snow cover have also been found in

the north-west of Scotland [11], suggesting that winter NAO− phases are associated with higher snowfall in these regions.

Whilst the magnitude of the NAOI is weaker in the summer months [12], significant NAOI-rainfall correlations have been reported [13]. However, the correlation coefficients are generally weaker in summer than during the winter months [10]. In winter, the NAO-rainfall response is characterised by a north-west/south-east spatial divide as described above, whilst in summer the spatial signature is more homogenous across the country [12,13]. In summer months, average monthly rainfall increases under NAO− conditions and decreases under NAO+ conditions are approximately 50–100 mm, compared to NAO neutral conditions [10].

These NAO rainfall signatures propagate through the hydrological cycle, with NAO responses observed across Great Britain in catchment runoff [14–16], groundwater [17,18] and fluvial water temperatures [19], although this propagation can be moderated by catchment characteristics such as topography, landcover and geology [15,16]. Ongoing research is exploring whether this understanding of NAO-rainfall-flow propagation can be incorporated into seasonal streamflow modelling and forecasting [20,21].

As discussed above, the NAO has been found to influence hydrometeorology across the country, and its spatial signature is evident in monthly average rainfall datasets [10]. However, several studies have reported inconsistency in seasonal NAO-rainfall responses across Great Britain. Hall and Hanna [13] present three winter rainfall anomaly maps produced by the UK Met Office for 2013/2014, 2014/2015 and 2015/2016 (see their Figure 1). The reported NAOI values all indicate an NAO+ phase of varying magnitudes. However, only in the winter of 2014/2015 was the typical north-west/south-east winter NAO-rainfall response (as described above) observed. This study concluded by foregrounding the role of other North Atlantic teleconnections as secondary modes of climate variability, such as the East Atlantic Pattern (EA) and Scandinavian Pattern, in influencing regional rainfall (and temperatures) in Britain [13]. Variability in winter NAO-rainfall signatures, both in terms of strength and spatiality, has also been attributed to other atmospheric teleconnections, in particular positive and negative phases of the EA, in other work [22,23].

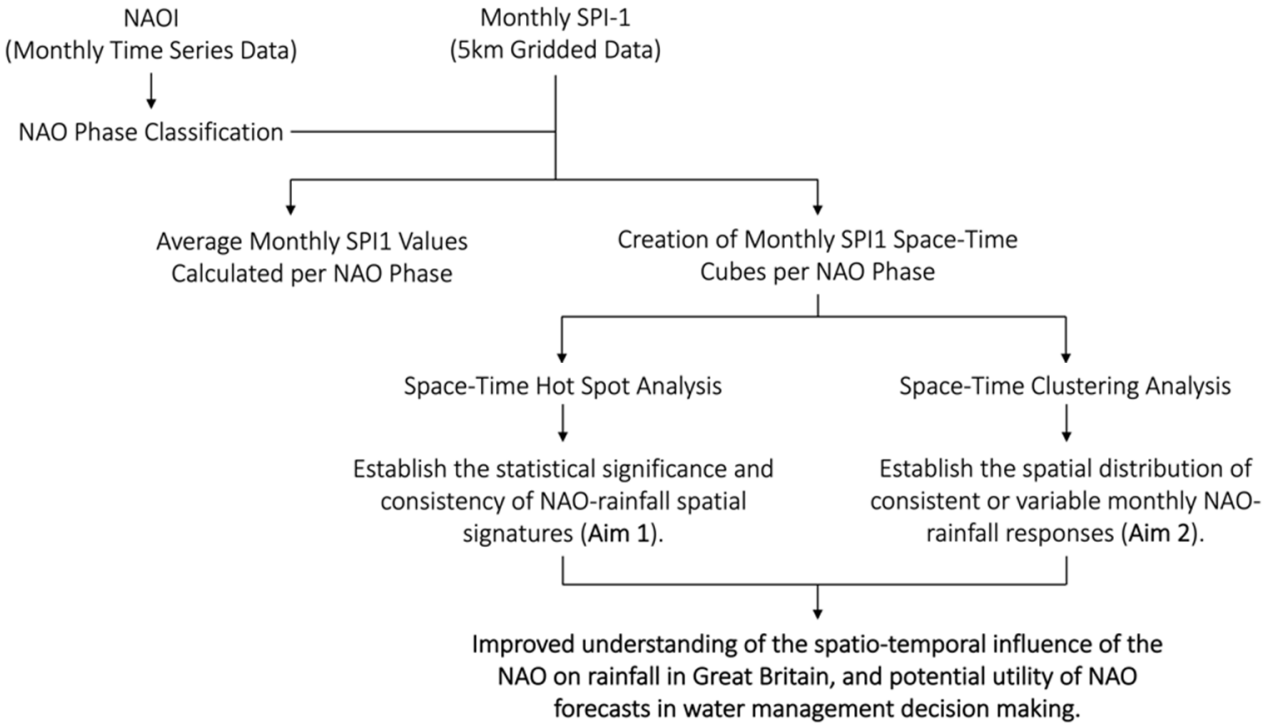

Figure 1. Flow chart of the analytical stages of this study.

Our ability to predict the NAO, especially during its stronger phases during the winter months [24,25], has improved. In particular, recent research from the National Center for Atmospheric Research (NCAR) and the UK Met Office suggests that winter NAO prediction several months in advance may be increasingly possible [26,27]. As NAO forecasting skill improves, it is important that we continue to develop our spatial and temporal understanding of the rainfall signatures associated with the circulation, especially as evidence of the propagation of NAO rainfall deviations to other hydrometeorological variables, such as runoff and groundwater, continues to emerge.

Whilst previous studies have explored average monthly and seasonal NAO-rainfall responses across Great Britain [1,10,13], as far as we are aware, no study has quantified the spatial influence of the NAO on rainfall distributions, and particularly the probability of wet and dry conditions/extremes. Understanding NAO-rainfall variability is important as it underpins the potential application of NAO forecasts in water management decision making. This study responds to this need through the novel application of spatio-temporal statistics and high spatial and temporal resolution Standardised Precipitation Index (SPI) data. Specifically, we aim to:

1. Assess the statistical significance and consistency of NAO-rainfall spatial signatures.
2. Establish the spatial distribution of consistent or variable monthly NAO-rainfall responses.

2. Materials and Methods

Figure 1 summarises the key stages of this analysis to explore space-time variability in monthly NAO-rainfall response across Great Britain, which are explained in full below.

2.1. Data

A range of indices have been used in previous work to quantify the phase and strength of the NAO [1,10,12,18], and the choice of NAOI can have a notable influence on subsequent analyses [28]. As this study focuses on quantifying monthly NAO-rainfall response variability across a full year, an NAOI calculated using a principal components (PC) analysis of the leading empirical orthogonal function of sea level pressure anomalies in the North Atlantic region was used [3]. These NAO indices avoid the limitation of indices directly derived using station-measured data in the summer months when the NAO dipoles can move away from the monitoring stations [28]. As a result, the use of station-based NAO indices in summer months can produce weaker and non-significant NAOI-rainfall correlation analyses [10]. Monthly PC-based NAOI data were downloaded for the period January 1900–December 2015 from NCAR [29].

Previous studies have used different approaches to defining NAO+ and NAO− phases using the NAOI. In this study, the NAO phase was defined as half the standard deviation plus/minus the long-term mean of the NAOI dataset [30]. By identifying NAO phases in this way, we could remove months where the NAO signal is weak, allowing only clear NAO+ and NAO− rainfall responses to be considered. NAO+ phases were defined as having a NAOI > 0.502 and NAO− < −0.503 (data between this range were classified as NAO neutral and removed). Table 1 shows the distribution of NAO phase and months for the period January 1900–December 2015.

We used the 5 km gridded Standardised Precipitation Index (SPI) dataset from the UK Centre for Ecology and Hydrology (CEH) [31] to represent precipitation. Standardised indices have been widely used in research exploring the hydrometeorological response to atmospheric-oceanic teleconnections [10,32,33]. The SPI dataset from CEH was calculated by fitting a gamma distribution to modelled historical rainfall using a standard period of 1961–2010 [31]. For this study, the SPI calculated with a one-month accumulation period (SPI-1) was used to give a relative indication of wetness/dryness compared to the standard period at a monthly scale. The SPI-1 data for the same period as the monthly NAOI from NCAR (January 1900–December 2015) were downloaded from CEH.

Table 1. Frequency Distribution of NAO Phases per Month (January 1900–December 2015).

Period	NAO+ Frequency	NAO− Frequency	NAO Neutral Frequency
Dec	47	40	29
Jan	52	36	28
Feb	47	40	29
WINTER	**146**	**116**	**86**
Mar	45	38	33
Apr	29	32	55
May	28	24	64
SPRING	**102**	**94**	**152**
Jun	26	24	66
Jul	16	16	84
Aug	16	19	81
SUMMER	**58**	**59**	**231**
Sep	19	21	76
Oct	31	33	52
Nov	29	31	56
AUTUMN	**79**	**85**	**184**

The SPI-1 values are normally distributed and can range from −5 to 5, although approximately 95% of values occur within the range of −2 (extremely dry) to 2 (extremely wet), and 68% within the range of −1 to 1 [31]. We use a qualitative classification of SPI-1 thresholds to indicate the relative degree of wetness/dryness (Table 2) in the interpretation of our results.

Table 2. Qualitative Descriptors for SPI-1 Values adapted from [34].

Qualitative Descriptor	SPI-1 Value Range
Extremely Wet	2.0–5.0
Very Wet	1.5–1.99
Moderately Wet	1.0–1.49
Near Normal	−0.99–0.99
Moderately Dry	−1.49–−1.0
Severely Dry	−1.99–−1.5
Extremely Dry	−5.0–−2.0

2.2. Calculation of Monthly Average SPI-1 Values

To provide a point of comparison, before undertaking the NAO-rainfall space-time variability analysis described below, we mapped the average monthly SPI-1 values under NAO+ and NAO− phases over the period January 1900–December 2015. The average monthly SPI-1 value under each phase was calculated for each 5 km pixel. This analysis provided a dataset of average rainfall conditions (represented by the SPI-1) for each calendar month under NAO+ and NAO− conditions.

2.3. Space-Time Data Array

To undertake the spatio-temporal analyses, the monthly SPI-1 data were structured into a series of data arrays (a space-time cube). Each array contained the monthly 5 km gridded SPI-1 data stacked in time ascending order for each NAO phase. The number of time steps in each space-time cube equalled the monthly-phase frequency values in Table 1. A space-time cube was created for each month under NAO+ and NAO− conditions using Esri ArcGIS Pro software (Version 2.6).

2.4. Space-Time Hot Spot Analysis (Getis Ord Gi Statistic)*

The Getis-Ord Gi* statistic [35] identifies clusters of significantly high and low values within a spatial dataset—identified as hot or cold spots with varying significance levels (90, 95 or 99%). The statistic indicates whether the spatial clustering of high/low values is

more pronounced than would be expected in a random spatial distribution of those same values [36]. The Getis-Ord Gi* statistic is commonly used in spatial statistical analyses in health and crime applications [37,38]. This study's application of it in the field of hydrometeorology/climatology is novel.

As the Getis-Ord Gi* statistic has a spatial component, its calculation requires consideration of how pixels are spatially related, so that high/low value clusters can be identified (i.e., a conceptualisation of spatial relationships between the 5 km SPI-1 pixels). Because of the spatially continuous gridded SPI-1 data, we used the 'edges and corners' or 'queens' contiguity rule, where each pixel's statistical neighbourhood included the eight pixels which share a boundary or point of contact in the four cardinal and diagonal directions. Hot spots in this context represent clusters of pixels where the SPI-1 values are significantly high, whilst cold spots represent the inverse (low SPI-1 values). The Getis-Ord Gi* statistic therefore allows for the identification of statistically significant wet or dry (high SPI-1/low SPI-1) spatial patterns.

The Getis-Ord Gi* statistic was calculated for each time step (SPI-1 dataset) in the space–time cubes for NAO+ and NAO− conditions. The output is a multi-variate dataset, indicating the percentage time each pixel is in either a significant hot (high SPI-1 value—wet) or cold spot (low SPI-1 value—dry). This enables an evaluation of the statistical significance and consistency of the spatial rainfall (wet/dry) response to the NAO across Great Britain and provides an assessment as to the spatial probability of significant wet/dry conditions under NAO+ and NAO− phases.

2.5. Space-Time Clustering Analysis

The second spatio-temporal analysis was a space-time clustering process [39], which grouped 5 km pixels with similar SPI-1 values across space, time, and NAO phase for each month. The clustering used a k-means algorithm with spatially random starting seeds. During the cluster calculation, SPI-1 time series similarity was assessed using the Euclidean distance between the SPI-1 time series values (the square root of the sum of squared differences in SPI-1 values across time) [39]. The algorithm produced 90 space-time clustering solutions, with potential results between two and ten output clusters. The optimal clustering solution was identified as that which had the highest pseudo-F statistic. This statistic describes the within-cluster SPI-1 time series similarity and between-cluster SPI-1 time series difference—the larger the pseudo-F statistic of the clustering solution, the greater the distinctiveness of each individual cluster in space and time [39].

The range of the average SPI-1 values within each space-time cluster was investigated using box plots, frequency histograms and descriptive statistics, quantifying the distribution of SPI-1 within clusters and providing a measure of the consistency/variability in space-time rainfall response to the phase of the NAO.

3. Results

3.1. Average Monthly SPI-1 Values

Figures 2 and 3 present the average monthly SPI-1 values under NAO+ and NAO− conditions. Whilst these are average monthly SPI-1 values and mask extreme values, clear spatial and temporal signatures of the NAO can be detected. In the winter months, the NAO rainfall response described in the introduction can be observed [1,7,12,13]. Under NAO+ conditions, the north-west areas have higher/positive average SPI-1 values, indicating wet conditions, and under NAO− conditions, the region is typically dry (negative SPI-1 values). The inverse average wet/dry response, albeit weaker, is seen in the southern and eastern areas.

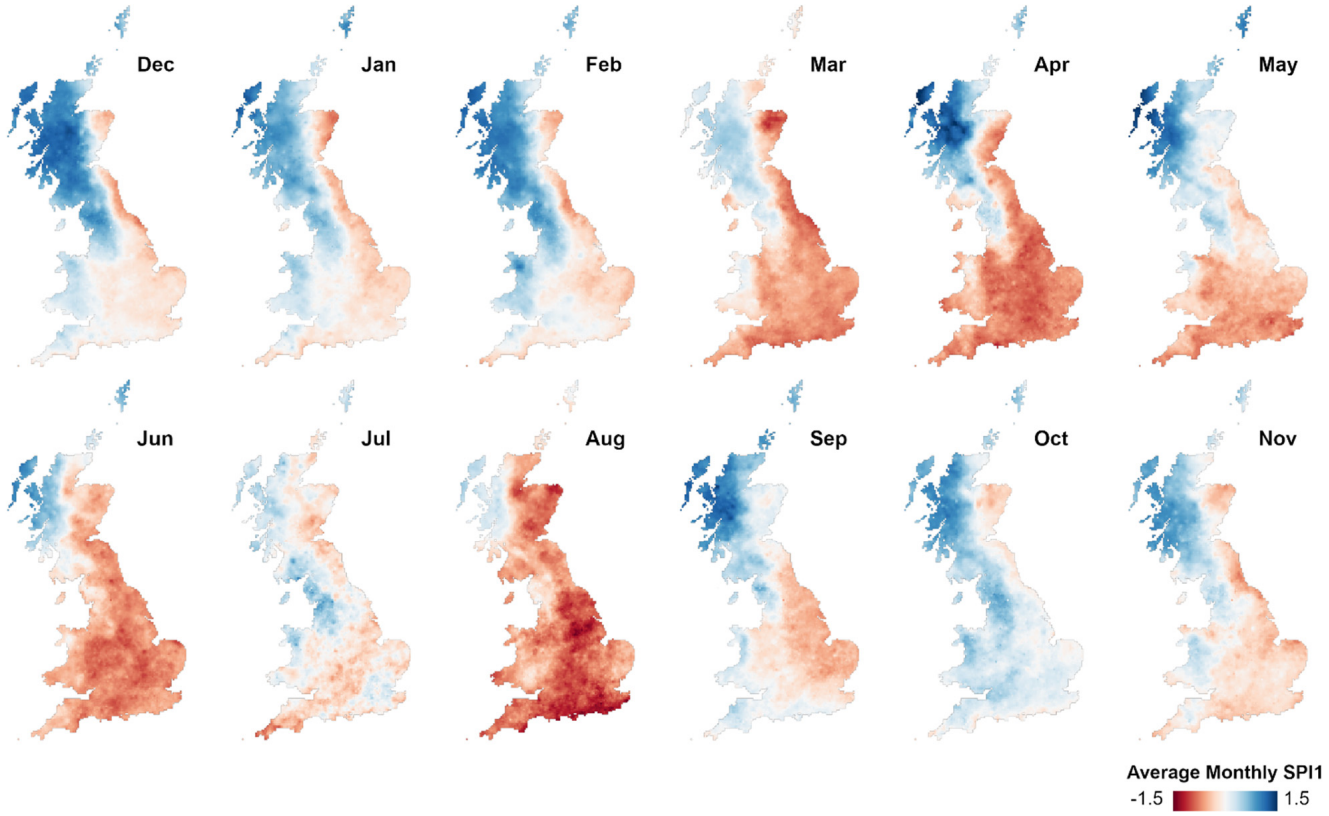

Figure 2. Average monthly SPI-1 values under NAO+ conditions (January 1900–December 2015).

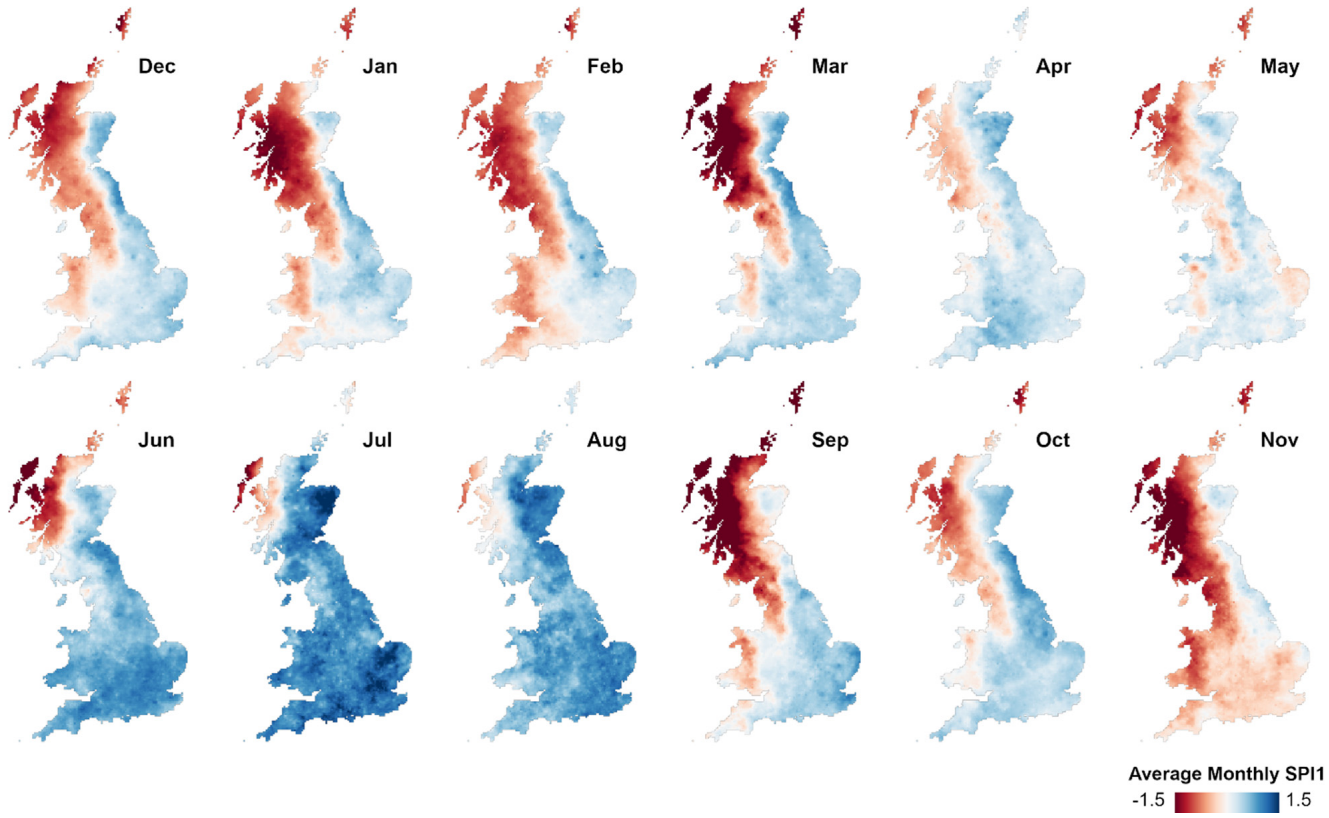

Figure 3. Average monthly SPI-1 values under NAO− conditions (January 1900–December 2015).

Moving through to the summer months, the average NAO-rainfall response becomes more spatially homogeneous (i.e., there is less difference between the different areas of the country), and the wet/dry response in the north-west during winter is inverted; a spatio-temporal pattern also noted in other studies [10,12,13].

3.2. Space-Time Hot Spot Results

Figures 4 and 5 show the results of the space-time hot spot analysis. This analysis involved calculating the Getis-Ord Gi* for each time step (SPI-1 dataset) of the month/phase space–time cubes as described in Section 2.3, allowing us to examine the statistical significance and consistency of the patterns discussed in Section 3.1 above. The mapped results in Figures 4 and 5 below show the percentage of time each 5 km pixel was in a statistically significant hot spot (i.e., a cluster of pixels with high/wet SPI-1 values) or cold spot (i.e., a cluster of pixels low/dry SPI-1 values). These maps indicate the spatial probability of significant wet/dry conditions under NAO+ and NAO− phases. Averages of these results for the nine Met Office Climate Districts for Great Britain are shown in Figure 6.

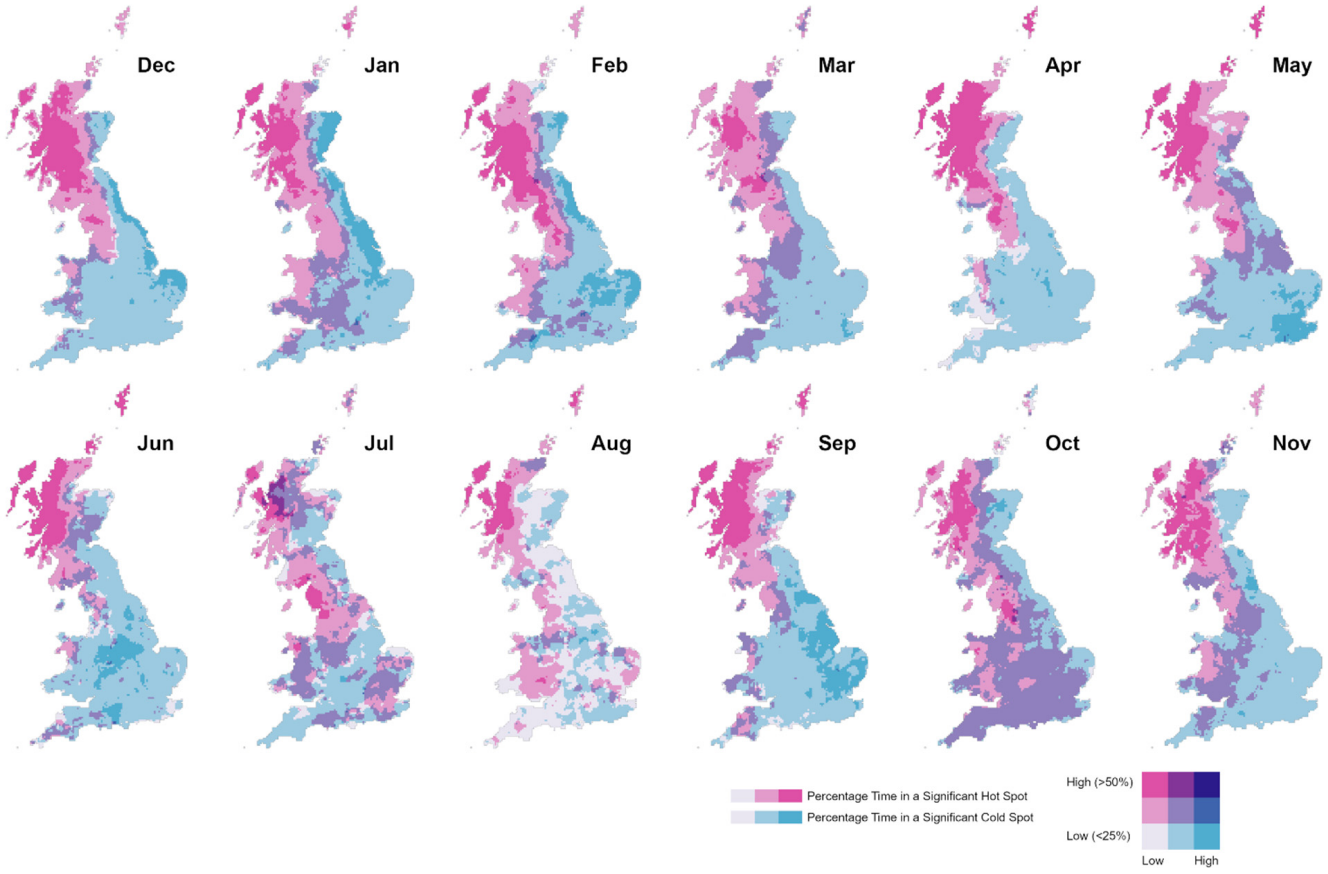

Figure 4. Space-time hot spot results under NAO+ conditions. Pinks indicate where the percentage of time in a significant hot spot is high (indicating wetter conditions), and light blues where the percentage of time in a significant cold spot is high (indicating drier conditions). Light grey indicates low occurrence of both hot and cold spots, whilst mixed shades indicate occurrence of both hot and cold spots. Disaggregated versions of these maps can be found in Appendix A.

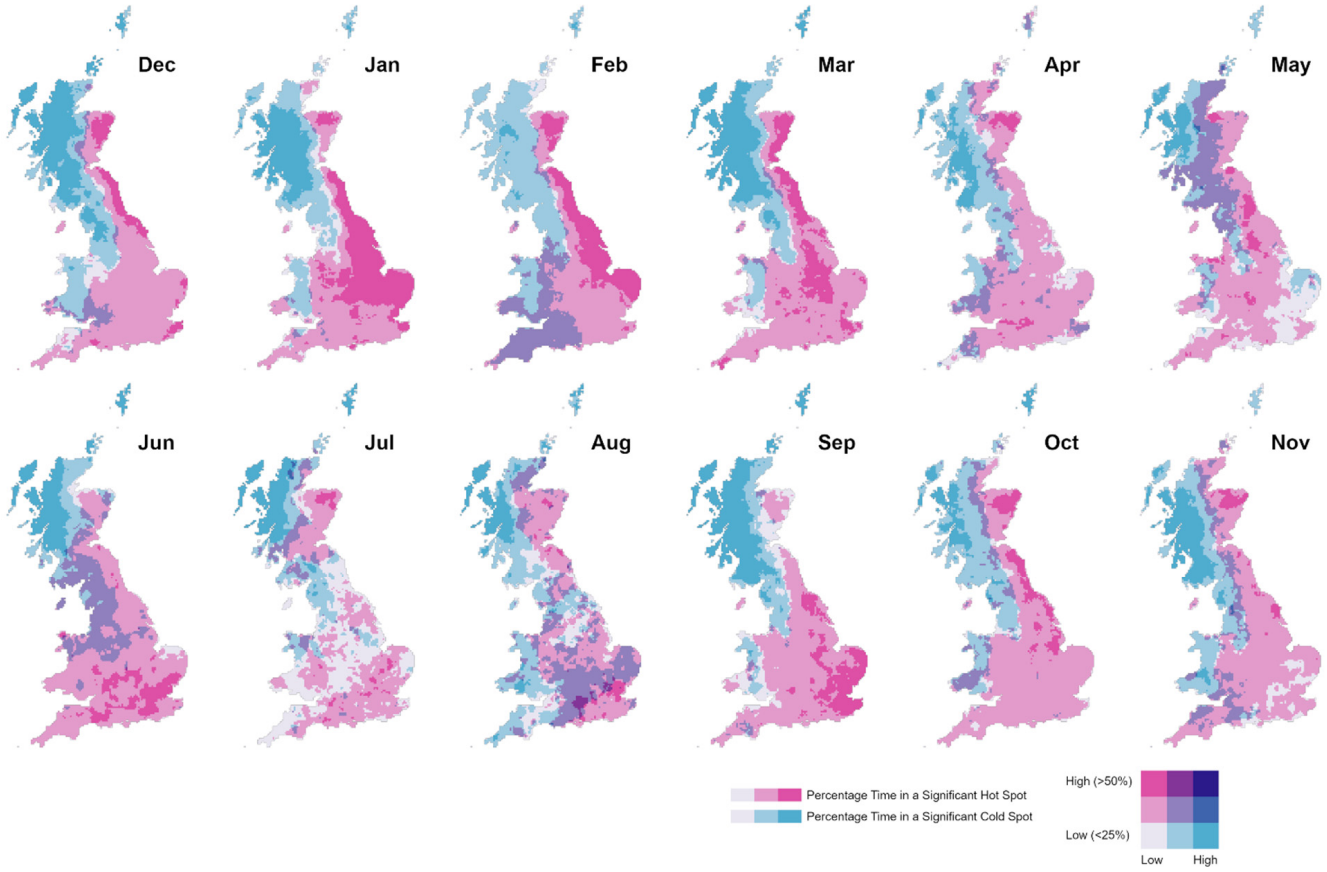

Figure 5. As per Figure 4 but under NAO− conditions.

The space-time hot spot analysis reveals statistically significant spatio-temporal patterns in the NAO-rainfall response across Great Britain. The winter months are marked by the previously noted north-west/south-east spatial divide of opposing wet/dry responses to the NAO, as identified in other studies [1,10,18]. In our analysis (Figures 4 and 5), this pattern is shown by the location of widespread hot and cold spots in the NW and SE areas, indicating significant clusters of pixels with high/low (wet/dry) SPI-1 values. This suggests that the wet/dry spatial pattern we detect in winter rainfall associated with the phase of the NAO is statistically significant.

Looking across the record, this NW/SE opposing response appears to have a relatively high degree of consistency in some areas, for example, Scotland North and West, and to a slightly lesser extent England South West and Central South and East Anglia are in a statistically significant wet/dry cluster (hot/cold spot) for a relatively high proportion of the analysis period (Figure 6). This suggests that there is a higher probability that the NAO+ and NAO− phases will result in this statistically significant winter NW/SE spatial pattern. However, it should be noted that in winter, some areas, for example Scotland East and England North West and Wales North, show little or no difference between the occurrence of significant clusters of wet/dry SPI-1 values (hot/cold spots). Therefore, the effect of the NAO in producing significant wet/dry spatial patterns in these Climate Districts is more limited.

Figures 2 and 3 show that the spatial rainfall response to the NAO is on average more homogeneous in the summer months [10,12,13]. As a result, less discernible patterns are found in the hot spot analysis, and the occurrence of statistically significant hot/cold spots (i.e., significant clusters of high/low SPI-1 values) is more variable in space and time (Figures 4 and 5). Most Climate Districts show minor differences in the occurrence of significant clusters of wet/dry SPI-1 values in summer, except for Scotland North and West (Figure 6).

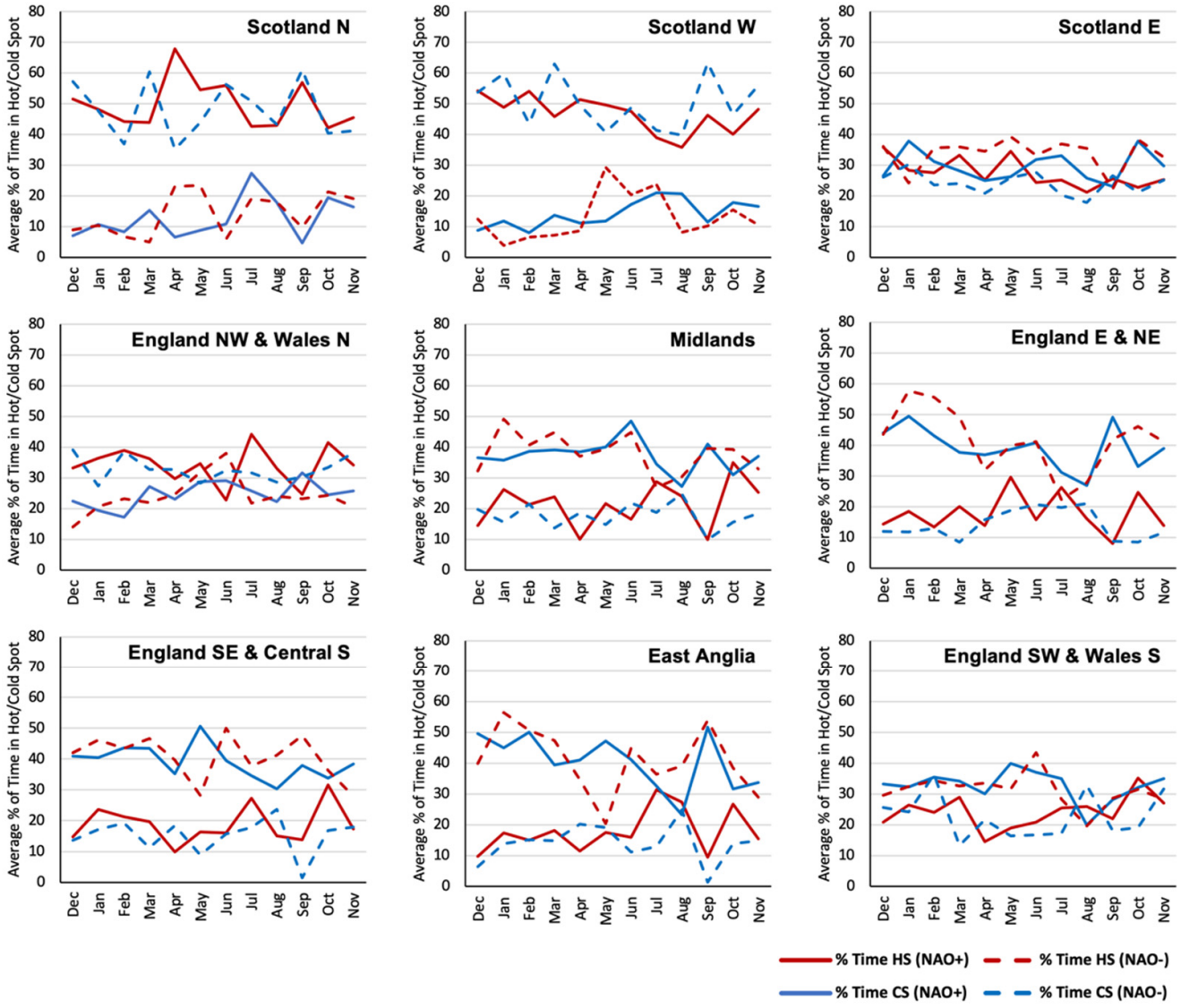

Figure 6. Regional average percentage of time in a significant hot/cold spot (based on the mapped results in Figures 4 and 5). Regions based on the Met Office Climate Districts for Great Britain.

3.3. Space-Time Clustering Results

Figures 7 and 8 present the space-time clustering results. This analysis explored the variability around the average NAO responses identified in Figures 2 and 3 (discussed in Section 3.1 above). Each cluster represents spatial groupings of 5 km pixels which have a similar response to the NAO phase during that month across the temporal record. The optimal number of clusters based on the pseudo-F statistic was consistently three. In Figures 7 and 8, the more saturated the blue/red colour, the more distinctive the space-time cluster wet/dry response to the NAO (i.e., the space-time median value is wetter/drier). Less saturated clusters indicate a space-time median SPI-1 value closer to 0, suggesting a less distinctive wet/dry average rainfall response to the NAO across the temporal record. The distributions of cluster median SPI-1 values per time step are plotted in Figure 9, and the associated descriptive statistics are shown in Figure 10. Figures 11 and 12 show frequency histograms of the cluster median SPI-1 values and the percentage of time each cluster experiences wet/dry conditions.

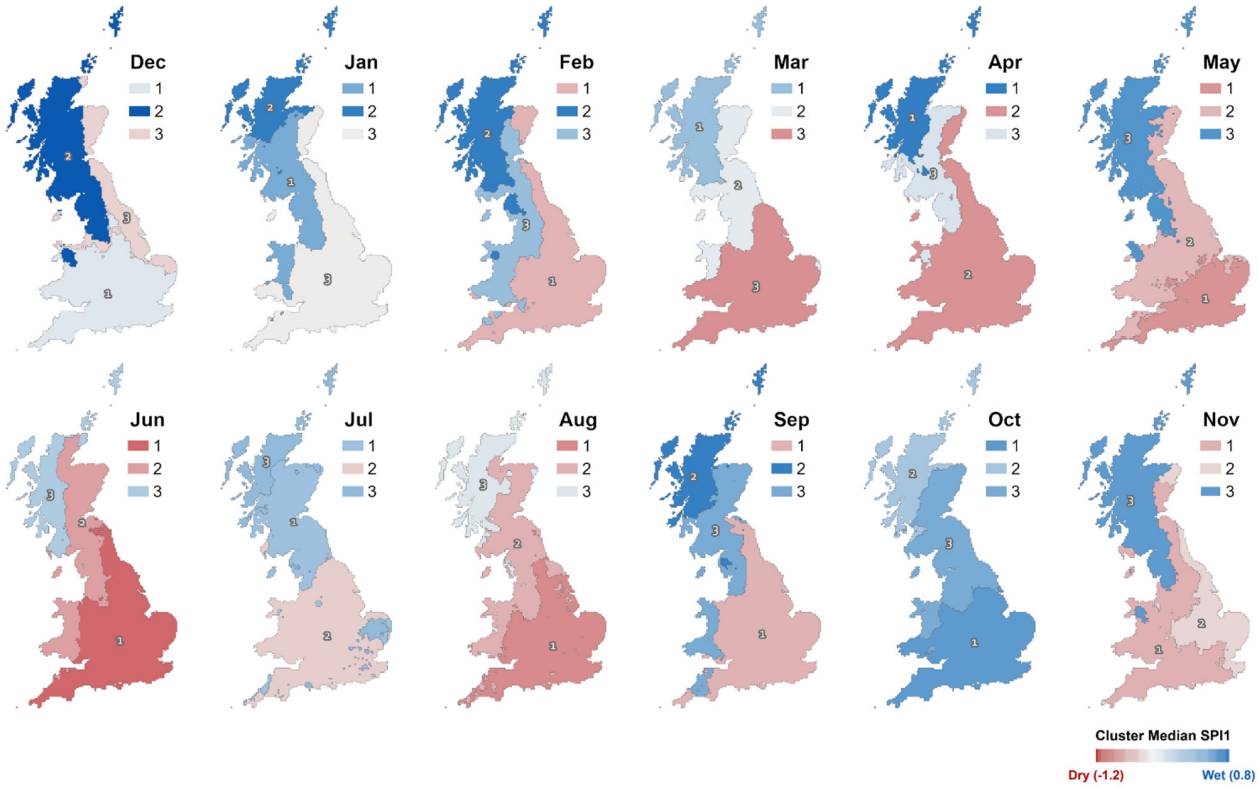

Figure 7. Monthly space-time clusters of SPI-1 values under NAO+ conditions. The clusters are coloured based on the median SPI-1 value of the cluster in space and time. Blue indicates a wetter median, whereas red indicates a drier median. Less saturated clusters indicate median SPI-1 values closer to 0.

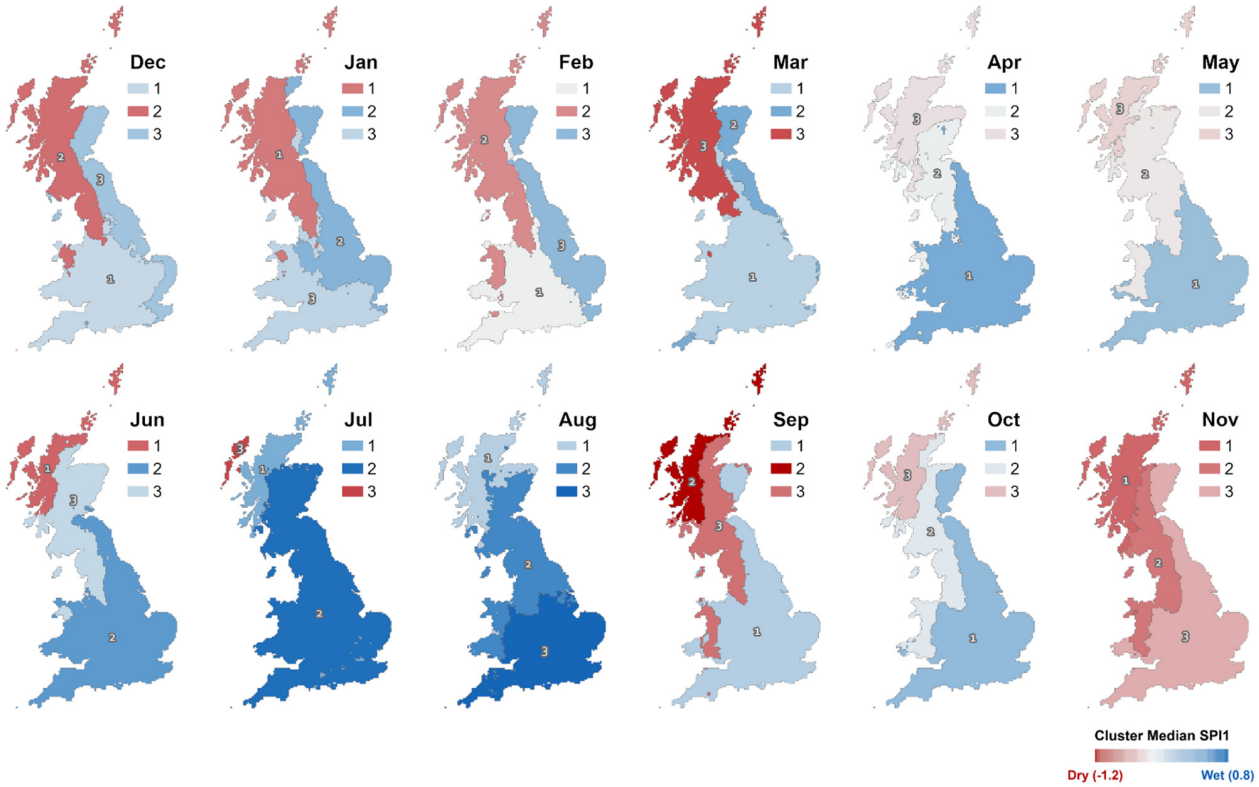

Figure 8. As per Figure 7 but showing the monthly space-time clusters of SPI-1 values under NAO− conditions.

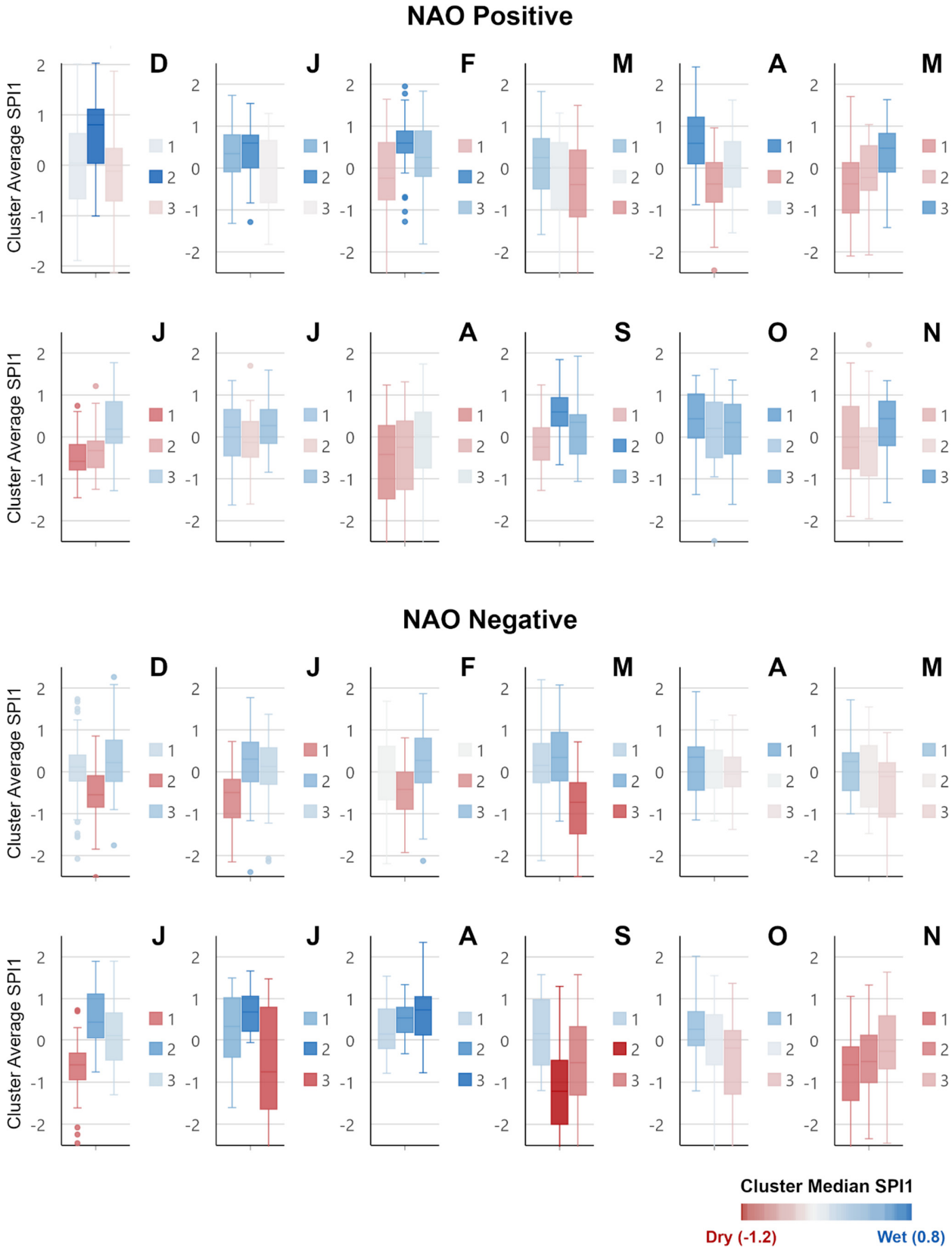

Figure 9. Box plots representing the distribution of cluster median SPI-1 values for the space-time clusters mapped in Figures 7 and 8. As with Figures 7 and 8 the box plots are coloured based on the median SPI-1 value of the cluster in space and time. Individual points represent outlier values.

	Dec NAO Positive			Dec NAO Negative		
	1	2	3	1	2	3
Median	0.044	0.802	-0.114	0.115	-0.551	0.219
Mean	-0.018	0.567	-0.101	0.072	-0.518	0.250
Minimum	-1.891	-1.009	-2.134	-0.208	-2.516	-1.755
Maximum	2.010	2.028	1.868	1.733	0.852	2.263
Range	3.901	3.037	4.002	1.941	3.367	4.018
First Quartile	-0.667	0.037	-0.711	-0.219	-0.844	-0.229
Third Quartile	0.631	1.114	0.335	0.400	-0.093	0.757
IQR	1.298	1.078	1.046	0.619	0.751	0.986
STD	0.966	0.740	0.920	0.905	0.742	0.822
Variance	0.933	0.547	0.846	0.819	0.551	0.675

	Jun NAO Positive			Jun NAO Negative		
	1	2	3	1	2	3
Median	-0.581	-0.326	0.184	-0.591	0.441	0.119
Mean	-0.468	-0.268	0.269	-0.684	0.530	0.172
Minimum	-1.453	-1.249	-1.286	-2.449	-0.762	-1.301
Maximum	0.742	1.213	1.770	0.726	1.895	1.897
Range	2.195	2.461	3.055	3.175	2.657	3.198
First Quartile	-0.788	-0.732	-0.150	-0.943	0.051	-0.479
Third Quartile	-0.183	-0.101	0.842	-0.312	1.110	0.658
IQR	0.605	0.631	0.992	0.631	1.060	1.137
STD	0.540	0.636	0.763	0.840	0.757	0.841
Variance	0.291	0.405	0.583	0.705	0.574	0.707

	Jan NAO Positive			Jan NAO Negative		
	1	2	3	1	2	3
Median	0.345	0.597	-0.010	-0.497	0.304	0.130
Mean	0.318	0.450	-0.093	-0.646	0.215	-0.037
Minimum	-1.321	-1.289	-1.821	-2.655	-2.395	-2.797
Maximum	1.736	1.541	1.305	0.719	1.771	1.373
Range	3.057	2.830	3.126	3.374	4.166	4.170
First Quartile	-0.089	0.004	-0.823	-1.097	-0.237	-0.301
Third Quartile	0.793	0.784	0.658	-0.179	0.707	0.571
IQR	0.882	0.780	1.481	0.918	0.944	0.872
STD	0.678	0.601	0.852	0.751	0.833	0.914
Variance	0.459	0.362	0.726	0.565	0.695	0.835

	Jul NAO Positive			Jul NAO Negative		
	1	2	3	1	2	3
Median	0.233	-0.133	0.268	0.338	0.683	-0.758
Mean	0.025	-0.072	0.087	0.265	0.656	-0.772
Minimum	-1.624	-1.603	-3.140	-1.606	-0.065	-4.827
Maximum	1.347	1.696	1.593	1.493	1.662	1.474
Range	2.971	3.298	4.733	3.099	1.727	6.300
First Quartile	-0.452	-0.484	-0.158	-0.413	0.223	-1.646
Third Quartile	0.655	0.363	0.652	1.023	1.060	0.796
IQR	1.107	0.848	0.809	1.436	0.836	2.442
STD	0.846	0.849	1.089	0.933	0.534	1.826
Variance	0.716	0.720	1.186	0.871	0.285	3.335

	Feb NAO Positive			Feb NAO Negative		
	1	2	3	1	2	3
Median	-0.240	0.598	0.250	0.005	-0.421	0.274
Mean	-0.117	0.568	0.286	-0.112	-0.541	0.232
Minimum	-2.610	-1.279	-0.257	-2.980	-3.149	-2.123
Maximum	1.642	1.950	1.835	1.682	0.813	1.864
Range	4.252	3.230	2.092	4.663	3.962	3.987
First Quartile	-0.758	0.359	-0.198	-0.667	-0.891	-0.261
Third Quartile	0.608	0.881	0.886	0.611	-0.006	0.804
IQR	1.367	0.522	1.084	1.279	0.885	1.065
STD	0.966	0.656	0.910	1.102	0.877	0.875
Variance	0.933	0.430	0.829	1.214	0.768	0.765

	Aug NAO Positive			Aug NAO Negative		
	1	2	3	1	2	3
Median	-0.422	-0.250	0.049	0.156	0.540	0.732
Mean	-0.568	-0.441	-0.087	0.242	0.487	0.556
Minimum	-2.837	-2.565	-2.554	-0.792	-0.330	-0.782
Maximum	1.238	1.314	1.739	1.539	1.337	2.344
Range	4.075	3.879	4.293	2.331	1.667	3.125
First Quartile	-1.478	-1.260	-0.744	-0.206	0.199	0.132
Third Quartile	0.271	0.379	0.588	0.756	0.796	1.050
IQR	1.749	1.639	1.333	0.963	0.597	0.918
STD	1.085	1.055	1.163	0.618	0.484	0.732
Variance	1.178	1.114	1.352	0.382	0.234	0.536

	Mar NAO Positive			Mar NAO Negative		
	1	2	3	1	2	3
Median	0.246	0.028	-0.394	0.153	0.342	-0.729
Mean	0.166	-0.190	-0.396	0.152	0.342	-0.819
Minimum	-1.587	-2.561	-2.899	-2.119	-1.180	-2.505
Maximum	1.826	1.313	1.495	2.198	2.071	0.716
Range	3.413	3.874	4.393	4.317	3.250	3.220
First Quartile	-0.496	-0.971	-1.164	-0.259	-0.218	-1.479
Third Quartile	0.704	0.607	0.426	0.677	0.941	-0.259
IQR	1.200	1.578	1.590	0.936	1.159	1.220
STD	0.803	0.995	1.097	0.848	0.721	0.818
Variance	0.644	0.990	1.204	0.718	0.520	0.669

	Sep NAO Positive			Sep NAO Negative		
	1	2	3	1	2	3
Median	-0.246	0.590	0.343	0.172	-1.219	-0.537
Mean	-0.169	0.581	0.161	0.193	-1.257	-0.502
Minimum	-1.280	-0.665	-1.064	-1.201	-3.027	-2.651
Maximum	1.238	1.840	1.923	1.575	1.295	1.574
Range	2.518	2.505	2.988	2.776	4.323	4.226
First Quartile	-0.556	0.255	-0.407	-0.589	-2.002	-1.306
Third Quartile	0.214	0.935	0.527	0.980	-0.483	0.334
IQR	0.770	0.680	0.934	1.569	1.518	1.640
STD	0.684	0.565	0.733	0.864	1.029	1.127
Variance	0.467	0.319	0.537	0.746	1.058	1.270

	Apr NAO Positive			Apr NAO Negative		
	1	2	3	1	2	3
Median	0.590	-0.380	0.062	0.349	0.010	-0.057
Mean	0.606	-0.459	0.052	0.215	0.007	-0.036
Minimum	-0.875	-2.754	-1.543	-1.150	-1.171	-1.375
Maximum	2.414	0.958	1.622	1.911	1.237	1.350
Range	3.289	3.712	3.165	3.061	2.408	2.725
First Quartile	0.100	-0.813	-0.456	-0.439	-0.392	-0.356
Third Quartile	1.215	0.134	0.632	0.593	0.514	0.352
IQR	1.116	0.947	1.088	1.032	0.906	0.708
STD	0.826	0.862	0.796	0.764	0.624	0.589
Variance	0.682	0.743	0.634	0.583	0.389	0.347

	Oct NAO Positive			Oct NAO Negative		
	1	2	3	1	2	3
Median	0.435	0.206	0.344	0.269	0.042	-0.197
Mean	0.428	0.106	0.161	0.306	-0.128	-0.503
Minimum	-1.375	-2.658	-1.610	-1.209	-2.646	-3.936
Maximum	1.467	1.617	1.355	2.014	1.550	1.368
Range	2.842	4.275	2.965	3.224	4.196	5.304
First Quartile	-0.028	-0.495	-0.406	-0.137	-0.591	-1.289
Third Quartile	1.023	0.829	0.781	0.691	0.621	0.240
IQR	1.051	1.323	1.186	0.828	1.213	1.529
STD	0.718	0.993	0.844	0.724	0.899	1.165
Variance	0.515	0.985	0.713	0.524	0.808	1.356

	May NAO Positive			May NAO Negative		
	1	2	3	1	2	3
Median	-0.377	-0.223	0.475	0.243	-0.027	-0.117
Mean	-0.384	-0.163	0.347	0.090	-0.046	-0.485
Minimum	-2.096	-2.072	-1.421	-1.007	-1.474	-2.544
Maximum	1.708	1.040	1.634	1.717	1.547	0.935
Range	3.804	3.111	3.056	2.724	3.021	3.479
First Quartile	-1.073	-0.534	-0.094	-0.452	-0.841	-1.081
Third Quartile	0.130	0.532	0.826	0.452	0.628	0.216
IQR	1.202	1.066	0.920	0.904	1.468	1.297
STD	0.901	0.852	0.705	0.648	0.881	0.985
Variance	0.811	0.725	0.497	0.421	0.776	0.971

	Nov NAO Positive			Nov NAO Negative		
	1	2	3	1	2	3
Median	-0.249	-0.101	0.434	-0.587	-0.512	-0.268
Mean	-0.075	-0.225	0.286	-0.815	-0.537	-0.131
Minimum	-1.899	-1.952	-1.568	-3.504	-3.628	-2.448
Maximum	1.766	2.201	1.344	1.058	1.327	1.634
Range	3.664	4.152	2.913	4.563	4.955	4.083
First Quartile	-0.763	-0.927	-0.209	-1.434	-1.013	-0.686
Third Quartile	0.723	0.216	0.849	-0.162	0.129	0.593
IQR	1.486	1.143	1.059	1.273	1.141	1.279
STD	0.902	0.937	0.734	1.032	1.115	0.972
Variance	0.814	0.879	0.538	1.066	1.244	0.944

Figure 10. Descriptive statistics for the space-time cluster median SPI-1 box plots in Figure 9 (IQR = interquartile range; STD = standard deviation). Formatting of colours is applied per statistical measure. Blue indicates wetter mean/median SPI-1 values, red indicates drier mean/median SPI-1 values. Green graduated shading indicates greater range/IQR values.

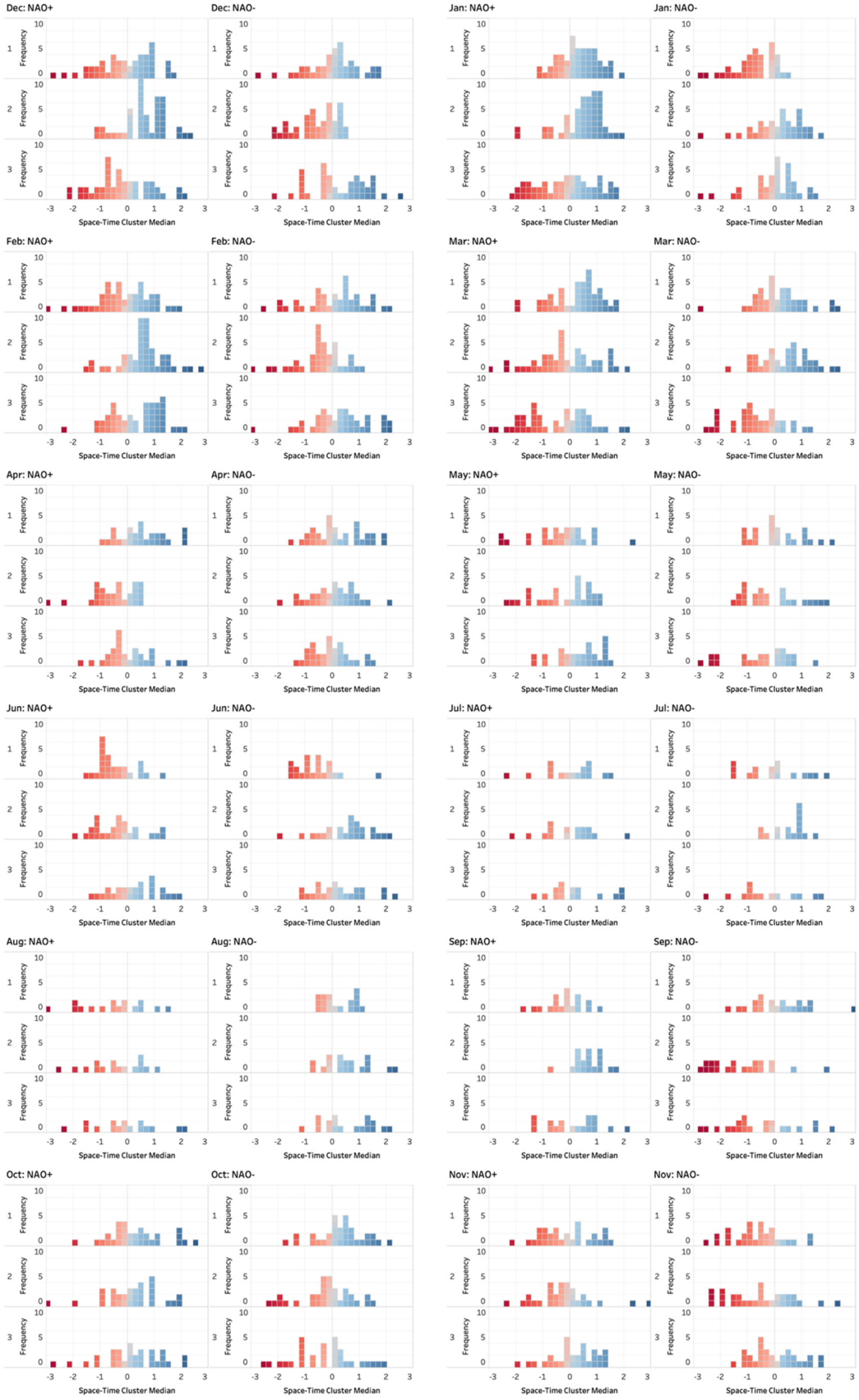

Figure 11. Frequency histograms of median SPI-1 values for the space–time clusters mapped in Figures 7 and 8.

	Cluster	Dry Conditions (%)	Wet Conditions (%)	Difference (%)
Dec NAO-	1	42.5	57.5	-15.0
	2	72.5	27.5	45.0
	3	45.0	55.0	-10.0
Dec NAO+	1	50.0	50.0	0.0
	2	17.4	82.6	-65.2
	3	60.9	39.1	21.7
Jan NAO-	1	83.3	16.7	66.7
	2	38.9	61.1	-22.2
	3	41.7	58.3	-16.7
Jan NAO+	1	30.8	69.2	-38.5
	2	21.2	78.8	-57.7
	3	51.9	48.1	3.8
Feb NAO-	1	40.0	60.0	-20.0
	2	70.0	30.0	40.0
	3	40.0	60.0	-20.0
Feb NAO+	1	53.2	46.8	6.4
	2	19.1	80.9	-61.7
	3	36.2	63.8	-27.7
Mar NAO-	1	47.4	52.6	-5.3
	2	36.8	63.2	-26.3
	3	78.9	21.1	57.9
Mar NAO+	1	33.3	66.7	-33.3
	2	57.8	42.2	15.6
	3	60.0	40.0	20.0
Apr NAO-	1	46.9	53.1	-6.3
	2	43.8	56.3	-12.5
	3	56.3	43.8	12.5
Apr NAO+	1	27.6	72.4	-44.8
	2	65.5	34.5	31.0
	3	55.2	44.8	10.3
May NAO-	1	50.0	50.0	0.0
	2	58.3	41.7	16.7
	3	54.2	45.8	8.3
May NAO+	1	60.7	39.3	21.4
	2	46.4	53.6	-7.1
	3	32.1	67.9	-35.7

	Cluster	Dry Conditions (%)	Wet Conditions (%)	Difference (%)
Jun NAO-	1	87.5	12.5	75.0
	2	29.2	70.8	-41.7
	3	41.7	58.3	-16.7
Jun NAO+	1	76.9	23.1	53.8
	2	73.1	26.9	46.2
	3	38.5	61.5	-23.1
Jul NAO-	1	50.0	50.0	0.0
	2	18.8	81.3	-62.5
	3	62.5	37.5	25.0
Jul NAO+	1	43.8	56.3	-12.5
	2	50.0	50.0	0.0
	3	50.0	50.0	0.0
Aug NAO-	1	50.0	50.0	0.0
	2	33.3	66.7	-33.3
	3	27.8	72.2	-44.4
Aug NAO+	1	68.8	31.3	37.5
	2	62.5	37.5	25.0
	3	62.5	37.5	25.0
Sep NAO-	1	47.6	52.4	-4.8
	2	90.5	9.5	81.0
	3	71.4	28.6	42.9
Sep NAO+	1	63.2	36.8	26.3
	2	5.3	94.7	-89.5
	3	42.1	57.9	-15.8
Oct NAO-	1	27.3	72.7	-45.5
	2	60.6	39.4	21.2
	3	51.5	48.5	3.0
Oct NAO+	1	45.2	54.8	-9.7
	2	38.7	61.3	-22.6
	3	38.7	61.3	-22.6
Nov NAO-	1	79.3	20.7	58.6
	2	62.1	37.9	24.1
	3	55.2	44.8	10.3
Nov NAO+	1	56.7	43.3	13.3
	2	66.7	33.3	33.3
	3	43.3	56.7	-13.3

Figure 12. Percentage of time the cluster median SPI-1 value is wet (positive SPI-1 values) and dry (negative SPI-1 values) based on the frequency histograms in Figure 11. The difference value represents the difference between the percentage of time under dry conditions and wet conditions.

3.4. Examples of Consistent Monthly NAO-Rainfall Responses

In the space-time clustering analysis, the NAO-rainfall response observed in the average monthly SPI-1 analysis (Figures 2 and 3) comes through clearly. For example, the north-west/south-east spatial divide in winter rainfall response [10] can be seen in Figures 4 and 5. During the winter months (DJF), the north-western areas experience the greatest change in rainfall under NAO+ and NAO− phases. In December, for example, the extremes of this response can be seen in NAO+ Cluster 2, which has a maximum cluster median SPI-1 value of 2 (extremely wet), and NAO− Cluster 2 which has a minimum cluster median SPI-1 value of −2.5 (extremely dry) (Figures 9 and 10).

Clusters covering these north-western areas in winter also show a relatively more consistent NAO-rainfall response compared to other parts of the country. For example, Dec NAO+ Cluster 2 has a 65% chance of being relatively wetter than drier, whilst the similarly located Dec NAO− Cluster 2 has a 45% probability of experiencing drier rather than wetter conditions (Figures 11 and 12). The interquartile range (IQR) of these two clusters also only include wet/dry cluster median SPI-1 values (Figure 9). Similar results for the north-western areas can be seen in January, for example the IQR for NAO− Cluster 1 only includes negative SPI-1 (dry) values (Figure 9).

In spring (MAM), similar spatial patterns to those described above can be seen, but with a north/south gradient in the clustering. As in winter, the median responses (Figures 7 and 8) match with the average monthly values mapped in Figures 2 and 3. For example, March NAO− Cluster 3 in north-western Scotland typically experiences notably dry conditions (Figure 8), with a 57% probability of experiencing drier rather than wetter conditions (Figures 11 and 12). This cluster also has a notably low minimum cluster median value of −2.5 representing extremely dry conditions.

In summer (JJA), the more spatially homogeneous wet/dry NAO−/NAO+ responses in Figures 2 and 3 can be seen in the cluster median values. Notably, the wet/dry di-

rectionality is the opposite to the NAO-rainfall response seen in the north-western areas during winter. For example, in June, NAO+ Clusters 1 and 2 which cover most of Great Britain (except for a cluster in the far north-west-Figure 7) show a relatively consistent dry response, with interquartile ranges (IQR) covering negative/dry SPI-1 values (Figure 9) and a 53% and 46% probability of drier rather than wetter conditions (Figures 11 and 12).

3.5. Examples of Variable Monthly NAO-Rainfall Responses

The space-time clustering analysis also reveals that whilst typical and relatively consistent NAO response signals can be observed, there is also significant NAO-rainfall response variability within some of the space-time clusters.

Even in areas that show relative consistency, variability in the cluster median SPI-1 values can still be observed (Figure 9). For example, in December, NAO− Cluster 2 in the north-western region (Figure 8), the minimum cluster median SPI-1 value is −2.5 which represents extremely dry conditions; however, the maximum is an SPI-1 value representing near-normal conditions (0.8). Whilst drier conditions are more likely in this cluster (72.5%), wet conditions were present for 27.5% of the time period analysed (Figures 11 and 12). In February, NAO+ Cluster 2, similarly covering the north-western area, the maximum cluster median SPI-1 value is 1.9 (severely wet) and the IQR covers positive values only. Whilst wetter than average conditions were found in this cluster for the majority of the time period (80%), the cluster did experience relatively dry conditions for 20% of the time period (Figures 11 and 12). These findings suggest that whilst the typical winter NAO responses can be observed in the north-western area, there is also some variability in both the magnitude of the NAO-rainfall response and the directionality (i.e., positive/wet, or negative/dry SPI-1 values).

The rainfall response in clusters covering the central, southern and eastern areas of Great Britain support the average winter NAO-rainfall response mapped in Figures 2 and 3. However, in comparison to the north-west, the winter rainfall response to NAO+ and NAO− phases is much more variable in clusters spanning these areas (Figures 7 and 8). For example, NAO+ Cluster 1 in December, has a notably large value range, with cluster median SPI-1 values ranging from a maximum of 2 (extremely wet) to −1.8 (severely dry) (Figures 9 and 10). The cluster median SPI-1 histograms also show a more normal distribution with more equal probability of relatively wet and dry conditions in this cluster (Figure 11). Similar variability in these areas can also be seen in January and February. Clusters spanning the central and southern areas of Britain (Figures 7 and 8) also show more variability in comparison to the north-west in spring.

In summer, some of the clusters covering the north-west exhibit more variability than similarly located clusters during the winter months. For example, June NAO+ Cluster 3 has a large cluster SPI-1 value range of −1.2 (moderately dry) to 1.7 (severely wet). Compared to the winter months in clusters covering the north-western area, the difference between the probability of wet and dry conditions associated with the phase of the NAO is reduced. In the example of June NAO+ Cluster 3, there is a 23% likelihood of experiencing wetter rather than drier conditions (Figures 11 and 12). Some clusters during the summer months have large SPI-1 value ranges (Figure 9), and the likelihood of relative wet/dry conditions is equally likely (Figure 12), for example July NAO+ Cluster 2 and August NAO+ Cluster 1, which span the central, southern and eastern areas of Great Britain.

In late summer, the average NAO-rainfall response across Great Britain can be notably strong in comparison to June and July [10]. Whilst this can be observed in the clustering analysis, there is variability in the magnitude of the NAO-rainfall response. For example, August NAO− Cluster 3 shows a 45% likelihood of wetter rather than drier conditions (Figure 12). However, the magnitude of these wet events can vary—the cluster average SPI-1 range varies from −0.7 (slightly dry, but near-normal) to 2.3 (extremely wet) (Figure 10), and the frequency histograms show a wider spread across positive SPI-1 values (Figure 11). This demonstrates that even when there are clear average signals,

as mapped in Figures 2 and 3, there can be significant spatio-temporal variability in the NAO-rainfall response.

4. Discussion

This study sought to evaluate the variability in NAO-rainfall response across Great Britain at high spatial and temporal scales. Average 5 km gridded SPI-1 values were mapped under NAO+ and NAO− conditions for the period January 1900–December 2015 (Figures 2 and 3). This revealed distinctive spatial signatures of the NAO in average monthly rainfall, such as the winter north-west/south-east spatial divide and more spatially homogeneous summer rainfall responses also observed in other studies [1,7,10,12,13]. The key spatio-temporal differences in NAO-rainfall response and relative consistency/variability between winter and summer revealed by our space-time analyses are summarised in Figure 13.

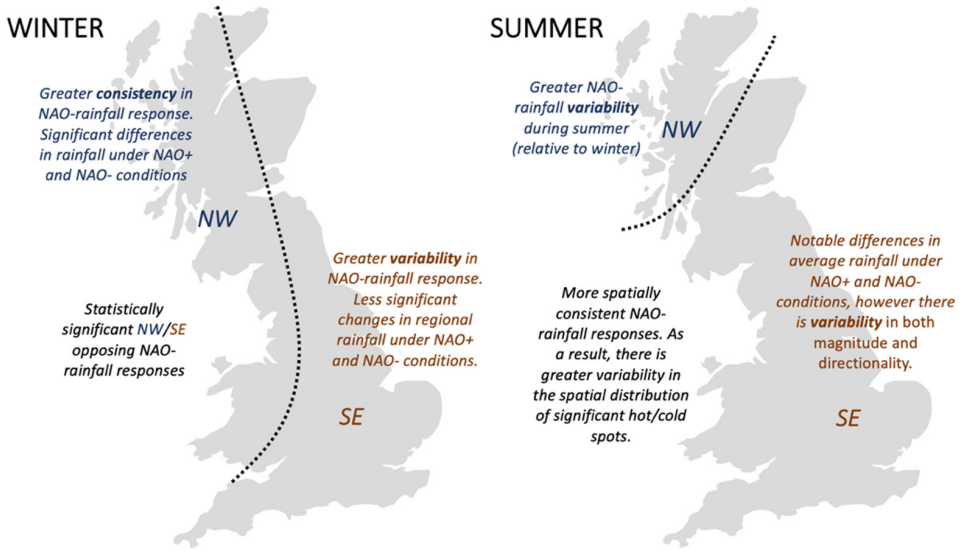

Figure 13. Schematic representation of the key spatio-temporal differences observed in NAO-rainfall response during the winter and summer months.

In the winter months, the results of the Getis-Ord Gi* space-time hot spot analysis confirm that the NW/SE spatial pattern (i.e., the spatial distribution of SPI-1 values) is statistically significant and consistent over the temporal record analysed (Figures 4 and 5). The space-time clustering analysis (Figures 7 and 8) also show these clear spatial patterns in the mean and median cluster average values, with clear differences as well in the frequency distribution of SPI-1 values related to NAO phase and region (Figures 11 and 12). This indicates a more spatially reliable estimate of monthly rainfall volume under NAO+ and NAO− phases may be possible during the winter months.

In the north-western areas of Great Britain, the space-time clustering and hot spot analyses reveal rainfall is very responsive to the phase of the NAO. There are clear differences in rainfall response between the two NAO phases, with values markedly fluctuating between wet (positive SPI- values) and dry (negative SPI-1 values) (Figure 9). Significant wet conditions occur under NAO+ conditions and dry conditions under NAO−, which supports the significant NAOI-rainfall correlations found in other studies [1,6,7,10]. Our space-time analyses show that the NAO-rainfall response in the north-western area during winter also shows greater consistency in these significant NAO+/NAO− wet/dry rainfall deviations. In some space-time clusters, the frequency histograms show that the probability of relative wetness/dryness differs significantly in the north-west during winter, for example Jan NAO− Cluster 1 has an 83% likelihood of experiencing dry conditions, whilst the similarly located NAO+ Clusters 1 and 2 have a 69% and 78% likelihood of wetter than average conditions (Figures 11 and 12). This indicates that we can have greater confidence

in how the monthly rainfall volume in the north-western area will change with the phase of the NAO during the winter months. Improved winter NAO forecasting skill [25–27] may therefore allow for effective water management decisions to be taken if we are able utilise this forecasting skill to predict an upcoming period of rainfall surplus (NAO+) or deficit (NAO−). However, it is important to note that even with these more consistent NAO-rainfall responses, our analysis shows the wet/dry response magnitude can still vary in the north-west (Figures 9 and 11).

The southern, eastern and central areas of Great Britain have a consistent opposing (wet/dry) NAO-rainfall response to the north-west during the winter months (Figures 4 and 5). However, the relative change in monthly average rainfall under NAO+ and NAO− conditions is notably less (Figures 2 and 3), with median space-time cluster values in these areas being closer to 0 (Figures 9 and 10). There is also greater variability in the NAO-rainfall response—the median SPI-1 histograms for clusters in these areas are typically more distributed across wet/dry values (Figure 11). The differences in the likelihood of relative wet/dry conditions associated with the phase of the NAO are notably reduced, being within approximately 20–30% (Figure 12). These findings suggest clear variability in both wet/dry event magnitude and directionality. As a result, it can be concluded that the NAO has a weaker and more variable influence on rainfall in the southern, eastern, and central areas, and as such, NAO forecasts might be of less practical use in water management decision making in comparison to the north-western area.

Differences in average monthly SPI-1 values during the summer months were found between the two NAO phases (Figures 2 and 3), and less distinctive spatial differences between the north-western and southern/central areas of the country were found [10,12,13] (Figures 4 and 5). The more spatially consistent rainfall patterns during summer may be associated with greater convective rainfall generation [10], compared to orographic rainfall during winter [16]. However, an area of future research would be to explore the physical processes resulting in the difference between NAO winter and summer rainfall patterns. On average, NAO+ conditions result in drier summer months, and NAO− wetter summer months (Figures 2 and 3) aligning with negative NAOI-rainfall correlations observed in other studies [10,12,13]. The median space-time cluster values corroborate this (Figure 10), and in some cases clusters show more distinctive wet/dry summer responses, with the differences in the likelihood of relative wetness/dryness being approximately 50% for some clusters over the time period analysed (Figure 12). However, other clusters across the country also show notable variability in terms of magnitude and directionality in the NAO-rainfall response (Figure 9), with the relative probability of relative wetness/dryness being equal in some clusters (Figure 12). These findings demonstrate that even with clear average monthly signals (Figures 2 and 3), there can be significant variability in the NAO-rainfall (wet/dry) response, which may limit the practicality of NAO forecasts for water management decision making during summer.

In summary, our space-time analyses reveal that whilst typical NAO-rainfall signatures can be observed across the year, there is also significant NAO-rainfall response variability in space and time. This variability in both rainfall magnitude and wet/dry directionality may be a limiting factor in the utility of incorporating NAO forecasts into water management decision making [40], even though the accuracy of these NAO forecasts has improved in recent years [25–27]. The exception being in the north-western area during winter, where significant and more consistent changes in rainfall [10,18], and subsequently catchment hydrology [16], can be found relatable to the phase and strength of the NAO.

Variability in NAO-rainfall response in space and time across Britain might be explained by other North Atlantic and European atmospheric-oceanic circulations (teleconnections) moderating or enhancing the rainfall effect of the NAO and/or being potentially more dominant in driving regional rainfall in areas where the NAO's effect is weaker or when the NAO is in a neutral phase. As discussed above, in our analysis, the central, southern and eastern regions of Great Britain frequently had relatively variable NAO-rainfall responses under NAO+ and NAO− phases. The East Atlantic pattern in particular has

been found to be positively correlated with rainfall these regions [13,41] and depending on its phase and strength may moderate or enhance the effect of the NAO on rainfall distribution and magnitude [22,23].

Our research supports the findings of Hall and Hanna [13], who suggest that even highly accurate NAOI forecasts might not provide enough information on their own to predict regional rainfall in Britain, and potentially subsequently catchment hydrology, several months in advance, without also considering the phase and magnitude of other atmospheric-oceanic circulations and climatic variables. As far as we are aware, no study has yet mapped at a high spatial and temporal (monthly) resolution the signature of these other North Atlantic/European circulations in regional rainfall across Great Britain.

In this study, the NAO was quantified using a PC-based NAOI, with phases defined using an approach adopted in previous work [10,30]. However, it is important to note that there is no universal approach to defining the NAO [42], and there is an opportunity for future work to explore the sensitivity of these results to the chosen NAOI and phase definition method. We have demonstrated the effectiveness of high resolution spatio-temporal analytical methods in exploring the meteorological impact of atmospheric circulations and revealing spatio-temporal climatic patterns. For example, the Getis-Ord Gi* statistic allowed for the identification of statistically significant spatial wet/dry patterns in the SPI-1 data in the winter months, although we acknowledge its limitation in detecting significant high/low value clusters in summer due to the more spatially consistent rainfall response. The space-time clustering analysis allowed us to look beyond average conditions and explore spatial and temporal consistency of the average and well-established NAO rainfall signatures in Great Britain. However, it is important to note that due to the random nature of the initial seed locations for the space-time clusters, modestly different results may be produced with a re-running of the analysis. This may be the case for locations (5 km pixels) where the spatial differences in the SPI-1 time series values are smaller and so may switch cluster membership between model runs, for example in the Midlands area between the more distinctive NW/SE zones during winter.

5. Conclusions

This study presents a novel application of space-time analyses to understand the variability in NAO-rainfall signatures at a high spatial (5 km) and temporal (monthly) resolution in Great Britain. Our analyses confirm that statistically significant NAO-rainfall signatures can be observed, and some regions show relatively high consistency in rainfall response to the phase of the NAO over time. However, our analyses also reveal that there is significant spatio-temporal variability in the rainfall response to the NAO, especially in the central, southern, and eastern areas of Great Britain. This has implications for the practical application of the NAOI in regional hydrometeorological forecasting as it is important to consider the variability in regional NAO-rainfall response under positive and negative phases of the NAO across Great Britain.

We suggest that such spatio-temporal variability might be explained by also considering the phase and magnitude of other atmospheric-oceanic teleconnections such as the East Atlantic Pattern. There is a need for high spatial and temporal resolution exploration of the hydrometeorological impact of these secondary modes of climate variability/teleconnections on rainfall in Great Britain, and in particular, the extent to which they might moderate or enhance the regional rainfall response to the NAO.

Author Contributions: Conceptualisation, H.W., N.Q. and M.H.; methodology, H.W., N.Q. and M.H.; software, H.W.; validation, H.W., N.Q. and M.H.; formal analysis, H.W.; investigation, H.W.; resources, H.W.; data curation, H.W.; writing—original draft preparation, H.W.; writing—review and editing, H.W., N.Q. and M.H.; visualisation, H.W., N.Q. and M.H.; supervision, N.Q. and M.H.; project administration, H.W. and N.Q. All authors have read and agreed to the published version of the manuscript.

Funding: This research received no external funding, and the APC was funded by the Department of Geography and Environmental Management at the University of the West of England, Bristol, UK.

Institutional Review Board Statement: Not applicable.

Informed Consent Statement: Not applicable.

Conflicts of Interest: The authors declare no conflict of interest.

Appendix A

Figure A1. Disaggregated space-time hot spot results (DJFM). Values indicate percentage of time in a statistically significant hot/cold spot.

Figure A2. Disaggregated space-time hot spot results (AMJJ). Values indicate percentage of time in a statistically significant hot/cold spot.

Figure A3. Disaggregated space-time hot spot results (ASON). Values indicate percentage of time in a statistically significant hot/cold spot.

References

1. Wilby, R.L.; O'Hare, G.; Barnsley, N. The North Atlantic Oscillation and British Isles climate variability, 1865–1996. *Weather* **1997**, *52*, 266–276. [CrossRef]
2. Rodwell, M.J.; Rowell, D.P.; Folland, C.K. Oceanic forcing of the wintertime North Atlantic Oscillation and European climate. *Nature* **1999**, *398*, 320–323. [CrossRef]
3. Hurrell, J.W.; Kushnir, Y.; Ottersen, G.; Visbeck, M. An overview of the North Atlantic Oscillation. In *The North Atlantic Oscillation: Climatic Significance and Environmental Impact*; American Geophysical Union: Washington, DC, USA, 2003; Volume 134, pp. 1–35.
4. Woollings, T.; Czuchnicki, C.; Franzke, C. Twentieth century North Atlantic jet variability. *Q. J. R. Meteorol. Soc.* **2013**, *140*, 783–791. [CrossRef]
5. Folwer, H.J.; Kilsby, C.G. Precipitation and the North Atlantic Oscillation: A study of climatic variability in Northern England. *Int. J. Climatol.* **2002**, *22*, 843–866.
6. Afzal, M.; Gagnon, A.S.; Mansell, M.G. Changes in the variability and periodicity of precipitation in Scotland. *Theor. Appl. Climatol.* **2015**, *119*, 135–159. [CrossRef]
7. Rust, W.; Holman, I.; Corstanje, R.; Bloomfield, J.; Cuthbert, M. A conceptual model for climatic teleconnection signal control on groundwater variability in Europe. *Earth Sci. Rev.* **2018**, *177*, 164–174. [CrossRef]
8. Simpson, I.R.; Jones, P.D. Analysis of UK precipitation extremes derived from Met Office gridded data. *Int. J. Climatol.* **2013**, *34*, 2438–2449. [CrossRef]
9. Kosanic, A.; Harrison, S.; Anderson, K.; Kavcic, I. Present and historical climate variability in South West England. *Clim. Chang.* **2014**, *124*, 221–237. [CrossRef]
10. West, H.; Quinn, N.W.; Horswell, M. Regional rainfall response to the North Atlantic Oscillation (NAO) across Great Britain. *Hydrol. Res.* **2019**, *50*, 1549–1563. [CrossRef]
11. Spencer, M.; Essery, R. Scottish snow cover dependence on the North Atlantic Oscillation index. *Hydrol. Res.* **2016**, *47*, 619–629. [CrossRef]
12. Folland, C.K.; Knight, J.; Linderholm, H.W.; Fereday, D.; Ineson, S.; Hurrell, J.W. The Summer North Atlantic Oscillation: Past, Present, and Future. *J. Clim.* **2009**, *22*, 1082–1103. [CrossRef]
13. Hall, R.J.; Hanna, E. North Atlantic circulation indices: Links with summer and winter UK temperature and precipitation and implications for seasonal forecasting. *Int. J. Climatol.* **2018**, *38*, e660–e677. [CrossRef]
14. Phillips, I.D.; McGregor, G.; Wilson, C.J.; Bower, D.; Hannah, D. Regional climate and atmospheric circulation controls on the discharge of two British rivers, 1974?97. *Theor. Appl. Climatol.* **2003**, *76*, 141–164. [CrossRef]
15. Rust, W.; Cuthbert, M.; Bloomfield, J.; Corstanje, R.; Howden, N.; Holman, I. Exploring the role of hydrological pathways in modulating North Atlantic Oscillation. *Hydrol. Earth Syst. Sci.* **2021**, *25*, 2223–2237. [CrossRef]
16. Burt, T.P.; Howden, N.J.K. North Atlantic Oscillation amplifies orographic precipitation and river flow in upland Britain. *Water Resour. Res.* **2013**, *49*, 3504–3515. [CrossRef]
17. Lavers, D.A.; Hannah, D.; Bradley, C. Connecting large-scale atmospheric circulation, river flow and groundwater levels in a chalk catchment in southern England. *J. Hydrol.* **2015**, *523*, 179–189. [CrossRef]
18. Rust, W.; Holman, I.; Bloomfield, J.; Cuthbert, M.; Corstanje, R. Understanding the potential of climate teleconnections to project future groundwater drought. *Hydrol. Earth Syst. Sci.* **2019**, *23*, 3233–3245. [CrossRef]
19. Wilby, R.; Johnson, M. Climate variability and implications for keeping rivers cool in England. *Clim. Risk Manag.* **2020**, *30*, 100259. [CrossRef]
20. UK Hydrological Outlook. UK Hydrological Outlook December 2020. Available online: http://www.hydoutuk.net/files/2816/0743/4122/2020_12_HO_Complete.pdf (accessed on 14 December 2020).
21. Donegan, S.; Murphy, C.; Harrigan, S.; Broderick, C.; Golian, S.; Knight, J.; Matthews, T.; Prudhomme, C.; Quinn, D.F.; Scaife, A.A.; et al. Conditioning Ensemble Streamflow Prediction with the North Atlantic Oscillation improves skill at longer lead times. *Hydrol. Earth Syst. Sci.* In Review. [CrossRef]
22. Comas-Bru, L.; McDermott, F. Impacts of the EA and SCA patterns on European twentieth century NAO−winter climate rela-tionship. *Q. J. R. Meteorol. Soc.* **2014**, *140*, 354–363. [CrossRef]
23. Mellado-Cano, J.; Barriopedro, D.; García-Herrera, R.; Trigo, R.M.; Hernández, A. Examining the North Atlantic Oscillation, East Atlantic Pattern, and Jet Variability since 1685. *J. Clim.* **2019**, *32*, 6285–6298. [CrossRef]
24. Weisheimer, A.; Schaller, N.; O'Reilly, C.; MacLeod, D.A.; Palmer, T. Atmospheric seasonal forecasts of the twentieth century: Multi-decadal variability in predictive skill of the winter North Atlantic Oscillation (NAO) and their potential value for extreme event attribution. *Q. J. R. Meteorol. Soc.* **2017**, *143*, 917–926. [CrossRef] [PubMed]
25. Parker, T.; Woollings, T.; Weisheimer, A.; O'Reilly, C.; Baker, L.; Shaffrey, L. Seasonal Predictability of the Winter North Atlantic Oscillation from a Jet Stream Perspective. *Geophys. Res. Lett.* **2019**, *46*, 10159–10167. [CrossRef]
26. Athanasiadis, P.J.; Yeager, S.; Kwon, Y.-O.; Bellucci, A.; Smith, D.W.; Tibaldi, S. Decadal predictability of North Atlantic blocking and the NAO. *npj Clim. Atmos. Sci.* **2020**, *3*, 1–10. [CrossRef]
27. Smith, D.M.; Scaife, A.A.; Eade, R.; Athanasiadis, P.; Bellucci, A.; Bethke, I.; Bilbao, R.; Borchert, L.F.; Caron, L.-P.; Counillon, F.; et al. North Atlantic climate far more predictable than models imply. *Nature* **2020**, *583*, 796–800. [CrossRef]
28. Pokorná, L.; Huth, R. Climate impacts of the NAO are sensitive to how the NAO is defined. *Theor. Appl. Clim.* **2015**, *119*, 639–652. [CrossRef]

29. National Centre for Atmospheric Research. Hurrell North Atlantic Oscillation Index (PC-Based). Available online: https://climatedataguide.ucar.edu/climate-data/hurrell-north-atlantic-oscillation-NAO$-$index-pc-based (accessed on 30 June 2020).
30. Berton, R.; Driscoll, C.T.; Adamowski, J.F. The near-term prediction of drought and flooding conditions in the northeastern United States based on extreme phases of AMO and NAO. *J. Hydrol.* **2017**, *553*, 130–141. [CrossRef]
31. Tanguy, M.; Fry, M.; Svensson, C.; Hannaford, J. *Historic Gridded Standardized Precipitation Index for the United Kingdom 1862–2015 (Generated using Gamma Distribution with Standard Period 1961–2010) v4*; NERC Environmental Information Data Centre: Wallingford, UK, 2017.
32. Irannezhad, M.; Haghighi, A.T.; Chen, D.; Klöve, B. Variability in dryness and wetness in central Finland and the role of teleconnection patterns. *Theor. Appl. Climatol.* **2014**, *122*, 471–486. [CrossRef]
33. Kingston, D.G.; Stagge, J.H.; Tallaksen, L.M.; Hannah, D.M. European-Scale Drought: Understanding Connections between Atmospheric Circulation and Meteorological Drought Indices. *J. Clim.* **2015**, *28*, 505–516. [CrossRef]
34. Djellouli, F.; Bouanani, A.; Babahamed, K. Climate change: Assessment and monitoring of meteorological and hydrological drought of Wadi El Hamman Basin (NW–Algeria). *J. Fundam. Appl. Sci.* **2016**, *8*, 1037–1053. [CrossRef]
35. Getis, A.; Ord, J.K. The Analysis of Spatial Association by Use of Distance Statistics. *Geogr. Anal.* **2010**, *24*, 189–206. [CrossRef]
36. Esri. Hot Spot Analysis (Getis-Ord Gi*). Available online: https://pro.arcgis.com/en/pro-app/latest/tool-reference/spatial-statistics/hot-spot-analysis.htm (accessed on 4 February 2021).
37. Ord, J.K.; Getis, A. Local Spatial Autocorrelation Statistics: Distributional Issues and an Application. *Geogr. Anal.* **1995**, *27*, 286–306. [CrossRef]
38. Scott, L.; Warmerdam, N. Extended Crime Analysis with ArcGIS Spatial Statistics Tools. Available online: https://www.esri.com/news/arcuser/0405/ss_crimestats1of2.html (accessed on 4 February 2021).
39. Esri. Space Time Cluster Analysis. Available online: https://pro.arcgis.com/en/pro-app/tool-reference/spatial-statistics/space-time-analysis.htm (accessed on 6 August 2020).
40. Rust, W.; Bloomfield, J.P.; Cuthbert, M.O.; Corstanje, R.; Holman, I.P. Non-stationary control of the NAO on European rainfall and its implications for water resource management. *Hydrol. Process.* **2021**, *35*, e14099. [CrossRef]
41. Casanueva, A.; Rodríguez-Puebla, C.; Frías, M.D.; González-Reviriego, N. Variability of extreme precipitation over Europe and its relationships with teleconnection patterns. *Hydrol. Earth Syst. Sci.* **2014**, *18*, 709–725. [CrossRef]
42. Hurrwll, J.W.; Deser, C. North Atlantic climate variability: The role of the North Atlantic Oscillation. *J. Mar. Syst.* **2009**, *78*, 28–41. [CrossRef]